

PAPER

The additive effects of photobiomodulation and bioactive glasses on enhancing early angiogenesis

To cite this article: Lidong Huang *et al* 2022 *Biomed. Mater.* **17** 045007

View the [article online](#) for updates and enhancements.

You may also like

- [Pulmonary blood mass dynamics on 4DCT during tidal breathing](#)
Nicholas Myziuk, Thomas Guerrero, Gukan Sakthivel *et al.*
- [Investigation of the Redox Behaviour of Double Perovskite PrBaMn₂O₆](#)
Andrea Felli, Alessandro Trovarelli and Marta Boaro
- [Impact of plant-based meat alternatives on cattle inventories and greenhouse gas emissions](#)
Jayson L Lusk, Dan Blaustein-Rejto, Saloni Shah *et al.*



Breath Biopsy[®] OMNI

The most advanced, complete solution for global breath biomarker analysis

SEE WHAT OMNI
CAN DO FOR YOU



Expert Study Design
& Management



Robust Breath
Collection



Reliable Sample
Processing & Analysis



In-depth Data
Analysis



Specialist Data
Interpretation

Biomedical Materials



PAPER

The additive effects of photobiomodulation and bioactive glasses on enhancing early angiogenesis

RECEIVED
2 December 2021

REVISED
18 April 2022

ACCEPTED FOR PUBLICATION
27 April 2022

PUBLISHED
13 May 2022

Lidong Huang^{1,3} , Weiyu Gong^{1,3}, Guibin Huang¹, Jingyi Li¹, Jilin Wu¹, Yuguang Wang^{2,*} and Yanmei Dong^{1,*}

¹ Department of Cariology and Endodontology, Peking University School and Hospital of Stomatology, Beijing, 100081, People's Republic of China

² National Engineering Laboratory for Digital and Material Technology of Stomatology, Peking University School and Hospital of Stomatology, Beijing 100081, People's Republic of China

³ Contributed equally to this study and should be considered joint first author.

* Authors to whom any correspondence should be addressed.

E-mail: kqdongyanmei@bjmu.edu.cn and young13doctor@163.com

Keywords: photobiomodulation, bioactive glasses, early angiogenesis, bone regeneration, tissue engineering

Abstract

Bioactive glasses (BG) have been widely utilized as a biomaterial for bone repair. However, the early angiogenesis of BG may be inadequate, which weakens its osteogenic effects in large-sized bone defects and often leads to the failure of bone regeneration. In this study, we explored the effects of photobiomodulation (PBM) combined with BG on early angiogenesis to solve this bottleneck problem of insufficient early angiogenesis. *In vitro*, human umbilical vein endothelial cells (HUVECs) were cultured with BG extracts and treated with PBM using 1 J cm^{-2} . The 3-(4,5-dimethylthiazol-2-yl)-2,5-diphenyltetrazolium bromide (MTT) assay, real-time reverse transcription-polymerase chain reaction (real-time RT-PCR) and tubule formation assay were utilized to detect HUVECs' proliferation, vascular growth factor genes expression and tubules formation. *In vivo*, bone defects at the femoral metaphysis in Sprague-Dawley rats were treated with BG particulates and PBM at 120 J cm^{-2} . Hematoxylin–eosin staining was used to observe the inflammatory response, tissue formation and biomaterial absorption of bone defects. Immunohistochemical staining was applied to observe the vascular-like structure formation. The *in vitro* results showed that PBM combined with BG significantly promoted HUVECs' proliferation, genes expression and mature tubules formation. On days 2, 4 and 7, the mRNA expression of VEGF in BG + PBM group was 2.70-, 2.59- and 3.05-fold higher than control ($P < 0.05$), and significantly higher than PBM and BG groups ($P < 0.05$). On days 4 and 7, the bFGF gene expression in BG + PBM group was 2.42- and 1.82-fold higher than control ($P < 0.05$), and also higher than PBM and BG groups ($P < 0.05$). Tube formation assay showed that mature tubules were formed in BG + PBM and PBM groups after 4 h, and the number in BG + PBM group was significantly higher than other groups ($P < 0.05$). *In vivo* results further confirmed PBM induced early angiogenesis, with more vascular-like structures observed in BG + PBM and PBM groups 2 week post-surgery. With the optimum PBM fluence and BG concentration, PBM combined with BG exerted additive effects on enhancing early angiogenesis.

1. Introduction

Bone grafting and biomaterial implantation are widely used for repairing large bone defects and fractures related to traumas, tumors and inflammatory diseases [1, 2]. Autografts, allografts and xenografts have a number of associated risks, such as donor deficiency, immunologic rejection and infection [3, 4].

Therefore, implantation of biomaterials has become an important method for bone defects repair [2]. As a biomaterial with good osteoconductivity and osteoinductivity, bioactive glasses (BG) have been widely clinically utilized [5, 6]. Studies have reported that BG is capable of promoting angiogenesis [7, 8], but it was also shown in one study that there were no significant differences in endothelial cell migration

at initial 5 h between nanosized BG group compared with the control group, probably due to the insufficient increase in the levels of vascular endothelial growth factor (VEGF), basic fibroblast growth factor (bFGF) and their receptor proteins in the early stage [9]. For this reason, it could be doubtful whether BG promotes the early migration of endothelial cells and enhances the early vascular network restoration, especially in *in vivo* situation that is relevant to the defect size, biomaterial morphology and ions release. Meanwhile, some literatures also pointed out that acute inflammatory reactions will occur when biomaterials are implanted, which will inhibit the angiogenesis process of osteoblasts and epithelial cells [10, 11]. The inadequate early angiogenesis of BG may result in insufficient nutrient supplies and harmful microenvironment changes, which weakens its osteogenic effects in large-sized bone defects repair, leading to ischemia and tissue necrosis in the central region of bone defects or ultimately the failure of bone regeneration [12, 13]. Therefore, inadequate angiogenesis is a problem that has created a bottleneck in tissue engineering. It is necessary to enhance the early angiogenesis of BG to further improve the quality and outcome of the large-sized bone defects repair.

Photobiomodulation (PBM) utilizes various forms of light sources, including light-emitting diodes and broadband lights in the visible and infrared spectrum, to elicit biostimulatory effects [14]. Studies have shown that PBM promotes angiogenesis [15–18]. The low-dose irradiation can activate endogenous chromophores, enhance the endothelial nitric oxide synthase (eNOS) synthesis, activate the mitogen-activated protein kinases (MAPKs) and other signal pathways, upregulate angiogenic-related growth factors, such as VEGF and bFGF [16], as well as stimulate endothelial cells' migration and proliferation [15–18]. Moreover, PBM has been reported to accelerate wound healing and newly bone formation [19]. Therefore, applying PBM may be helpful to promote the early angiogenic ability of BG and accelerate bone repairing.

In recent years, some studies have combined PBM and biomaterials to observe their effects on wound healing and tissue regeneration. Several studies achieved good results and found that PBM improved bone repair process together with biomaterials [20–23]. In other studies, however, the combination of PBM and biomaterials did not show the expected effects of promoting tissue regeneration [24–27]. Therefore, there is still no consistent conclusion whether the advantages of PBM can be applied positively with biomaterials. In addition, most of these studies applied the *in vivo* experiments, however, *in vitro* experiments were also important to first determine whether the combination of PBM and BG could generate additive effects and what were the contributing factors. Therefore, we used *in vitro* experiments to preliminarily explore the promoting

effects of PBM combined with BG on endothelial cells' proliferation, proangiogenic genes expression and tubules formation. Then we verified their additive effects on early angiogenesis by observing the enhancement in angiogenic-related proteins expression and vascular-like structures formation *in vivo*, aiming to provide a foundation for further investigations on their combined applications in bone regeneration.

2. Materials and methods

2.1. Cell culture

Primary human umbilical vein endothelial cells (HUVECs, ScienCell, Los Angeles, CA, USA) were cultured in endothelial cell medium (ECM, ScienCell, Los Angeles, CA, USA) containing basal medium with 5% fetal bovine serum, 1% endothelial cell growth supplement and 1% penicillin-streptomycin at 37 °C with 5% CO₂ (SERIES II, ThermoForma, Waltham, MA, USA). The medium was changed every other day. The HUVECs between passages 5 and 7 were used for experiments.

2.2. Preparation of BG particulates and ionic extracts

The BG used in this study was PSC (22.7% P₂O₅, 48.2% SiO₂ and 29.1% CaO (wt%)) which was produced with a sol-gel method using phytic acid as the precursor [28, 29]. To prepare the BG ionic extracts, BG particulates were sterilized at 180 °C for 4 h and then immersed to ECM in gradient concentrations of 0.01, 0.1, 1 and 2 mg ml⁻¹. The suspensions were shaken at 100 rpm at 37 °C for 24 h and filtered through a 0.22 μm filter. Then 5% fetal bovine serum, 1% endothelial cell growth supplement and 1% penicillin-streptomycin were added to the ionic extract ECM to obtain the BG culture medium.

2.3. Parameter settings and application of PBM therapy

The laser utilized in the study was an 808 nm near-infrared semiconductor laser with the 6–12 W output power in the continuous-wave mode (LWIRL808 nm, Beijing Laserwave Optoelectronics Technology Co., Ltd.). The distance between optical fiber and culture plate surface was adjusted to fix the spot size at 4 cm in diameter. The actual irradiance received was adjusted to 50 mW cm⁻², which was verified by a power meter. The irradiation time was calculated as irradiation time (s) = fluence (J cm⁻²)/irradiance (W cm⁻²). During irradiation, aluminum foil was used to cover the untreated wells of the cell culture plates so that the actual irradiance spot size was defined by the size of window on the aluminum-foil to make sure that the exposed wells could be irradiated evenly. The parameters of PBM *in vitro* and *in vivo* were listed in table 1.

Table 1. The parameters of PBM therapy.

Parameters	MTT	PCR & Tubule formation	<i>In vivo</i>
Mode	CW ^a	CW ^a	CW ^a
Irradiance (mW cm ⁻²)	50	50	200
Fluence (J cm ⁻²)	0.5, 1, 3, 5	1 ^b	120
Time of irradiation (s)	10, 20, 60, 100	20	600
Spot size (cm)	4	4	1.3
Distance of tip and tissues (cm)	9.8	9.8	2

^a CW, continuous-wave.

^b The fluence of PBM in RT-PCR and tubules formation assay was the optimum fluence identified by the MTT assay.

2.4. HUVEC proliferation assay

2.4.1. Proliferation of HUVECs cultured in different concentrations of BG extracts

HUVECs (80%–90% confluence) were digested using 0.25% trypsin-EDTA (Invitrogen, Carlsbad, CA, USA), centrifuged and prepared into single cell suspension. The HUVECs were seeded into 96 well plates at 3000 cells/well with five replicates per group. After a 24 h incubation, the medium was replaced with BG extracts of gradient concentrations (0.01, 0.1, 1 and 2 mg ml⁻¹). HUVECs cultured in ECM without BG extracts served as the control group. The medium was changed every 2 d. On days 1, 3, 5, 7 and 10, the 3-(4,5-dimethylthiazol-2-yl)-2,5-diphenyltetrazolium bromide (MTT, Sigma-Aldrich, St. Louis, MO, USA) assay was performed to observe the cells' proliferation. The optical density (OD) values were measured at a wavelength of 490 nm by a microplate reader (ELX808, BioTek, Winooski, VT, USA). The BG concentration of the group with the highest OD value was selected as the optimum concentration.

2.4.2. Proliferation of HUVECs cultured with different fluences of PBM

HUVECs were cultured in ECM at 3000 cells/well with five replicates per group and treated with gradient light dosages (0.5, 1, 3 and 5 J cm⁻²). Parameters of PBM were listed in table 1. Aluminum foil was used to cover the plate and light was delivered to 1 well of 96 well plate each time. HUVECs cultured in ECM without PBM were served as the control group. Medium was changed every 2 d. PBM was applied on days 0, 1 and 2 after cells were seeded. MTT assay was performed on days 1, 3, 5, 7 and 10. The PBM fluence of the group with the highest OD value was selected as the optimum fluence.

2.4.3. Proliferation of HUVECs exposed to PBM combined with BG extracts

HUVECs were seeded in 96 well plates with five replicates per group. After incubated for 24 h, the cells were divided into four groups: BG + PBM group (HUVECs cultured in ECM containing BG extracts and receiving PBM in the first 3 d); PBM group (HUVECs cultured in ECM and receiving PBM in the

first 3 d); BG group (HUVECs cultured in ECM containing BG extracts); and control group (HUVECs cultured in ECM). The BG extracts in this experiments was the ECM containing BG extracts of the optimum concentration determined by the previous experiments. Media were changed every 2 d. On days 0, 1 and 2, the BG + PBM and PBM groups received PBM of the optimum fluence identified by the previous experiments (table 1). The MTT assay was performed on days 1, 3, 5, 7 and 10.

2.5. Gene expression assay of VEGF and bFGF by real-time reverse transcription-polymerase chain reaction (real-time RT-PCR)

HUVECs were seeded into 6 well plates at the density of 1.0×10^5 cells/well, 0.8×10^5 cells/well and 0.5×10^5 cells/well respectively, divided into four groups (BG + PBM group, PBM group, BG group and control group) and treated respectively as described above. The cells in the BG + PBM and PBM groups received PBM on days 0, 1 and 2 (table 1). On days 2, 4 and 7, cells were lysed using TRIzol (Invitrogen, Carlsbad, CA, USA) and the total RNA was extracted. Reverse transcription was conducted using the FastStart Universal SYBR Green Master reverse transcription kit (Roche, Indianapolis, IN, USA). The cDNA was synthesized using 2.0 µg total RNA of each group in a 20 µl reaction system. The primer sequences are shown in table 2. All the reactions started with an initial denaturation step at 50 °C for 2 min and 95 °C for 10 min, followed by 40 cycles of PCR, comprising denaturation for 15 s at 95 °C and annealing/extension for 60 s at 60 °C. Two parallel samples were tested, and experiments were performed in triplicate. Data were analyzed by the $2^{-\Delta\Delta C_t}$ method. Glyceraldehyde 3-phosphate dehydrogenase (GAPDH) was used as the housekeeping gene to quantify relative gene expression. A fold change was defined as the relative gene expression compared to the value of the control group on day 2.

2.6. HUVEC tubule formation assay

50 µl Matrigel matrix (Becton, Dickinson and Company, Piscataway, NJ, USA) was added per well to laser scanning confocal microscope specific 96 well

Table 2. The primers sequences for real-time RT-PCR.

Primers	Sequences
VEGF	Forward: 5'-GCAAGAAATCCCGTCCCT-3' Reverse: 5'-TCGTTAACTCAAGCTGCCTC-3'
bFGF	Forward: 5'-AAGAGCGACCCTCACATCA-3' Reverse: 5'-TCGTTTCAGTGCCACATAACC-3'
GAPDH	Forward: 5'-CAACGGATTGGTTCGTA TTGG-3' Reverse: 5'-GCAACAATATCCACTTTACCAG AGTTAA-3'

plates (JingAn, Shanghai, China) and incubated at 37 °C for 45 min. The group division was the same as above. Cells of different groups were seeded on the matrix at 3×10^4 cells/well with three replicates per group. For the BG + PBM and BG groups, HUVECs were suspended in ECM containing BG extracts. Then, the BG + PBM and PBM groups received PBM (table 1). After 4 and 10 h, cells were stained by the Live/Dead cell staining kit (Sigma-Aldrich, St. Louis, MO, USA) and observed under a laser scanning confocal microscope (FV1200, Olympus, Tokyo, Japan). Nine random fields of each well were photographed and the images were analyzed with the Image J 1.8.0. A complete closed loop was considered as a tubular structure surrounded by many individual HUVECs. Complete tubules in the random fields could be automatically identified by the software and the number of tubules were counted. The branches, which indicated HUVECs had not formed complete tubular structures, were not included in the total number.

2.7. *In vivo* animal surgeries and experiments

Bone defects in the distal metaphysis of both femurs of the Sprague Dawley rats were chosen as the *in vivo* animal model. Twelve healthy Sprague Dawley rats, 12 week-old with weight about 500 g, were provided by the Central Laboratory of Peking University Stomatology Hospital and qualified for quarantine. Ethics approval for animal experiments was obtained from the Biomedical Ethics Committee of Peking University (LA2016309). Rats were randomly numbered from 1 to 12 with 24 femurs samples in total, of which six samples were randomly assigned to each group respectively. During surgery, rats were intraperitoneally injected with 5% chloral hydrate for anesthesia (0.7 ml/100 g). Then, a 2 cm-long incision starting from the lateral knee joint and bisecting along the angle was made. After the distal metaphysis of femur were exposed, cylindrical defects with 3 mm in diameter and 3 mm in depth were drilled at the metaphysis. Bone defects of the BG + PBM and PBM groups were treated with PBM. The vertical distance between the optical fiber and the bone defect was 2 cm and the laser spot were adjusted to cover the bone defect completely. The laser irradiance was

200 mW cm⁻² and lasted for 10 min. Therefore, the fluence that the bone defects received each time was 120 J cm⁻² (table 1). In the BG + PBM and PBM groups, the PBM was performed 3 times in total. The first time PBM operation was conducted before filling the BG particulates into the bone defects. Then bone defects were filled with BG particulates in the BG + PBM and BG groups while the bone defects of the PBM and control groups were only filled with blood clots. Then the soft tissue was sutured with 4–0 silk thread. The second and third time PBM were carried out on the first- and second-days post-surgery with an interval of 24 h. Tramadol (5 mg kg⁻¹) was injected intramuscularly for analgesia, and penicillin (100 000 UI ml⁻¹, 1 ml kg⁻¹) was injected consecutively for 3 d to prevent the infection.

2.8. Hematoxylin–eosin staining (HE staining)

Two weeks post-surgery, samples were obtained and fixed in 4% paraformaldehyde. After decalcified in 10% EDTA, dehydrated and embedded in paraffin, slices with the thickness of 5 µm were prepared. The direction was perpendicular to the defect surface and parallel to the long axis of femur. Slices were deparaffinized with xylene and rehydrated in a graded ethanol series. Then, dye the slices with hematoxylin for 15 min and use running water to wash off floating color. 1% hydrochloric acid alcohol was used for 2 s for differentiation. Then, wash the slices with distilled water. Eosin dyed the slices for 1 min and distilled water washed the slices for 30 s. After that, the slices were successively immersed in 70% ethanol, 80% ethanol, 90% ethanol, 95% ethanol, anhydrous ethanol, xylene, and then sealed with neutral gum. The inflammatory response, tissue formation and biomaterial absorption of bone defects were observed under a microscope (BX51, Olympus, Deutschland GmbH, Hamburg, Germany).

2.9. Immunohistochemical assay of CD105 and CD34

Two weeks post-surgery, samples were obtained and fixed in 4% paraformaldehyde. After decalcified in 10% EDTA, dehydrated and embedded in paraffin, slices with the thickness of 5 µm were prepared. The direction was perpendicular to the defect surface and parallel to the long axis of femur. Slices were deparaffinized with xylene and rehydrated in a graded ethanol series. 3% hydrogen peroxide was utilized to eliminate endogenous peroxidase and then samples were rinsed in phosphate buffer solution (PBS) 3 times for 10 min each time. Antigen retrieval was performed by rinsing samples in protease K (P9460, Solarbio, Beijing, China) for 15 min. Then, samples were rinsed in PBS 3 times for 10 min each time and blocked in 0.5% goat serum at room temperature for 40 min. The

primary antibody, CD105 (Proteintech, Cat# 10862-1-AP, RRID: AB_2098906, Chicago, IL, USA) diluted 1:200 or CD34 (Proteintech, Cat# 60180-1-Ig, RRID: AB_10733337, Chicago, IL, USA) diluted 1:1000 in PBS, was added and incubated at 4 °C overnight. Then, samples were processed with the anti-rat/rabbit universal immunohistochemical detection kit (Proteintech, Chicago, IL, USA). The secondary antibody, anti-rat/rabbit HRP labelled polymer, was incubated with the samples for 30 min at 37 °C. After rinsed with PBS, samples were chromogenically imaged using DAB, stained in hematoxylin and flushed with water. The vascular-like structures labelled by CD105 and CD34 were observed under a microscope (BX51, Olympus, Deutschland GmbH, Hamburg, Germany).

2.10. Statistical analysis

All the experiments were performed at least three times. Statistical analysis was performed with SPSS 22.0 (SPSS Inc., IL, USA) using one-way ANOVA for overall analysis of the cell proliferation, real-time RT-PCR and tubule formation experiments. The LSD test was used for group comparison, and the Kruskal–Wallis *H* test was performed when variance was uneven. $P < 0.05$ indicates statistically significant differences.

3. Results

3.1. PBM combined with BG promoted HUVECs proliferation

The MTT assay was performed to detect the effect of different BG extract concentrations on HUVECs' proliferation. The cell proliferation in 0.1 mg ml⁻¹ group was significantly higher than that of the control group on days 5 and 7 ($P < 0.05$). The OD value of 0.1 mg ml⁻¹ group on day 7 was the highest of all the experimental groups with significant differences ($P < 0.05$). 1 mg ml⁻¹ also remarkably promoted HUVECs' proliferation compared to the control group on day 5 ($P < 0.01$). However, there were no significant differences among 1 mg ml⁻¹, 2 mg ml⁻¹ and 0.01 mg ml⁻¹ groups on days 5 and 7. Moreover, the OD value of 2 mg ml⁻¹ group was significantly lower than that of the control group on day 10 ($P < 0.01$), indicating an inhibitory effect on cell proliferation. There was no significant difference between the 0.01 mg ml⁻¹ group and the control group at all time points (figure 1(a)).

The effect of PBM fluence on HUVECs' proliferation was also observed (figure 1(b)). PBM of 1 J cm⁻² showed the most promoting effect on cell proliferation. The OD values of the 1 J cm⁻² group were significantly higher than those of all other groups on days 5 and 7 ($P < 0.05$). For the 3 J cm⁻² and 5 J cm⁻² groups, the OD values were remarkably higher than those of the control group on days 3 and 5 ($P < 0.05$) but displayed an obvious decline on day 10. The

0.5 J cm⁻² group showed enhanced cell proliferation only on day 5 ($P < 0.01$). There were no significant differences among 0.5 J cm⁻², 3 J cm⁻² and 5 J cm⁻² groups on days 5 and 7.

Based on these previous results, the optimum BG + PBM parameters were determined as 0.1 mg ml⁻¹ BG extracts and 1 J cm⁻² PBM fluence, which were applied in the following experiments (figures 1(c) and (d)). On day 5, the BG + PBM group exhibited significantly promoted proliferation compared to the BG group ($P = 0.01$) and the control group ($P < 0.01$). On day 7, the OD value of the BG + PBM group was the highest compared to those of the PBM group ($P = 0.02$), BG group ($P < 0.01$) and control group ($P < 0.01$).

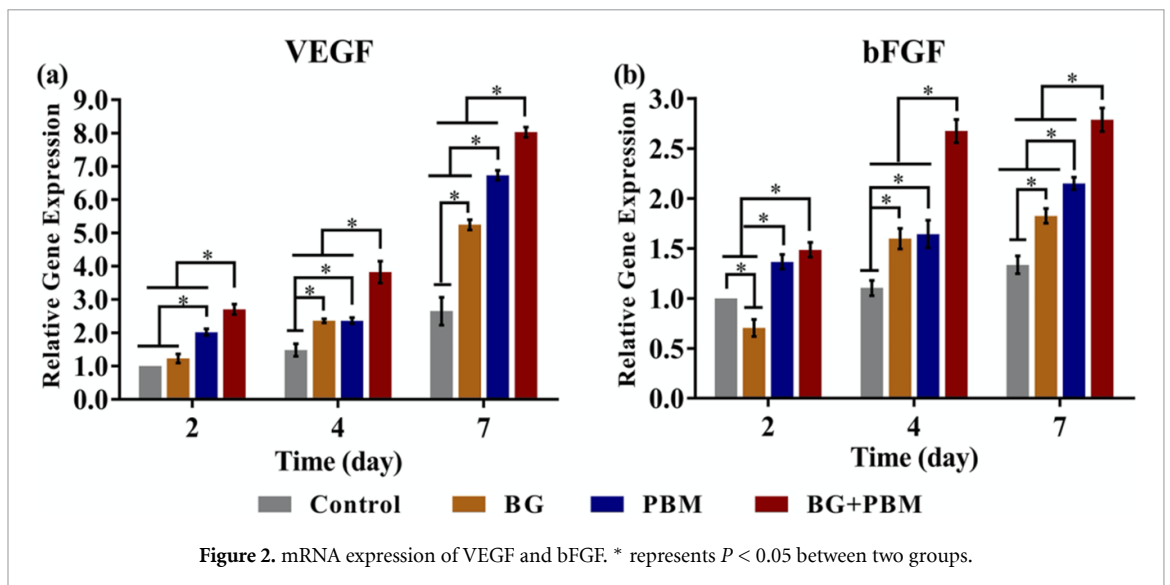
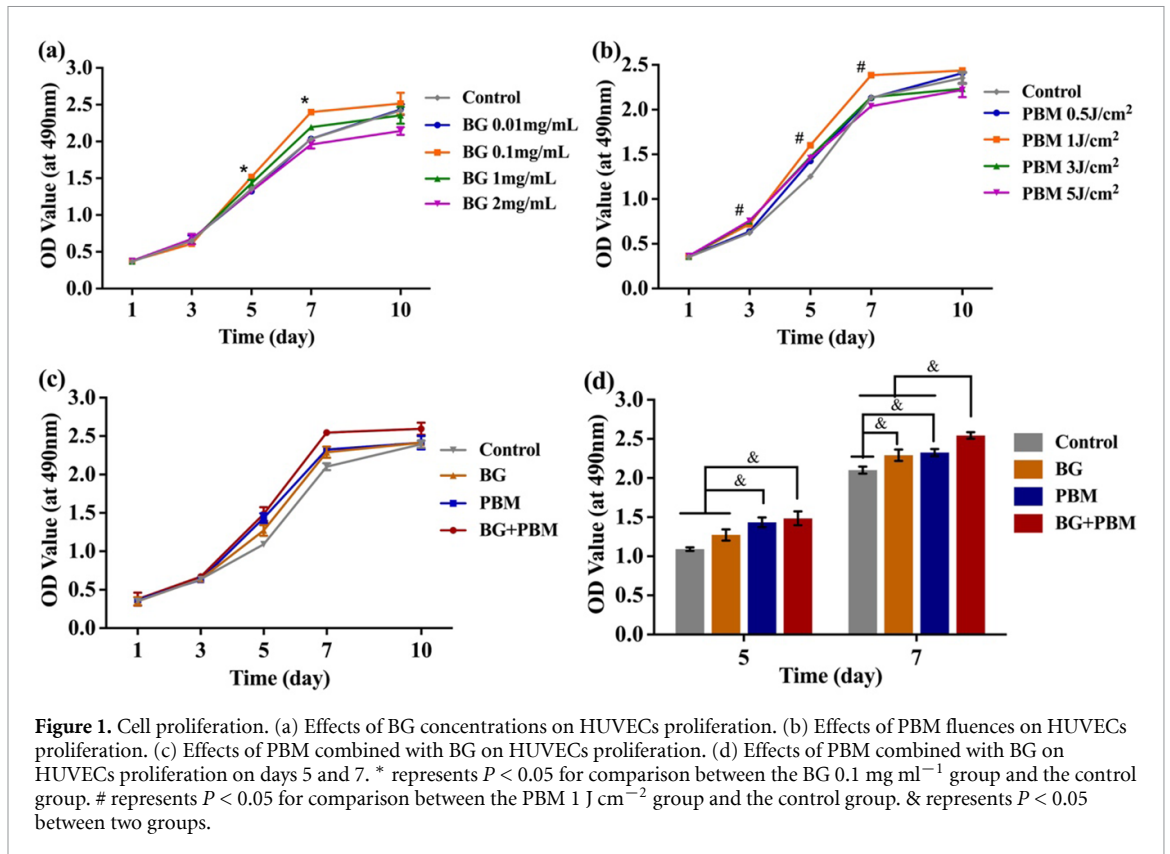
3.2. PBM combined with BG promoted genes expression of angiogenic-related growth factors

The VEGF gene expression in the BG + PBM group was 2.70-, 2.59- and 3.05-fold higher than that of the control group on days 2, 4 and 7 ($P < 0.01$), respectively, which was also significantly higher than those of the PBM and BG groups ($P < 0.05$). The PBM group also showed significantly upregulated VEGF gene expression compared to the BG and control groups at all time points ($P < 0.05$). The BG group showed significantly increased VEGF expression on days 4 ($P = 0.02$) and 7 ($P < 0.01$) compared with the control group but was less than those of the BG + PBM and PBM groups (figure 2).

On days 4 and 7, the bFGF gene expression in the BG + PBM group was 2.42- and 1.82-fold higher than that of the control group ($P < 0.01$), respectively, and also significantly higher than those of the PBM and BG groups ($P < 0.01$). The bFGF gene expression in the PBM group was significantly enhanced on day 2 compared with the control group ($P < 0.01$) and on day 7 compared with the BG group ($P < 0.01$). The BG group also showed higher bFGF gene expression on day 4 ($P = 0.01$) and 7 ($P = 0.018$) than the control group, but lower than the BG + PBM and PBM groups (figure 2).

3.3. PBM combined with BG promoted HUVEC tubule formation

At 4 h, a large number of complete and mature tubules formed in the BG + PBM and PBM groups (figure 3). Less complete tubules were observed in the BG group with some uncoupled branches. Cells in the control group primarily formed stacking-like structures. Quantitative analysis with Image J showed that significantly more tubules were formed in the BG + PBM and PBM groups than in the BG and control groups ($P < 0.05$). The BG + PBM group showed more tubules formation than the PBM group. At 10 h, complete tubules formed in all groups. The BG + PBM group formed the most tubules among all the groups ($P < 0.05$).



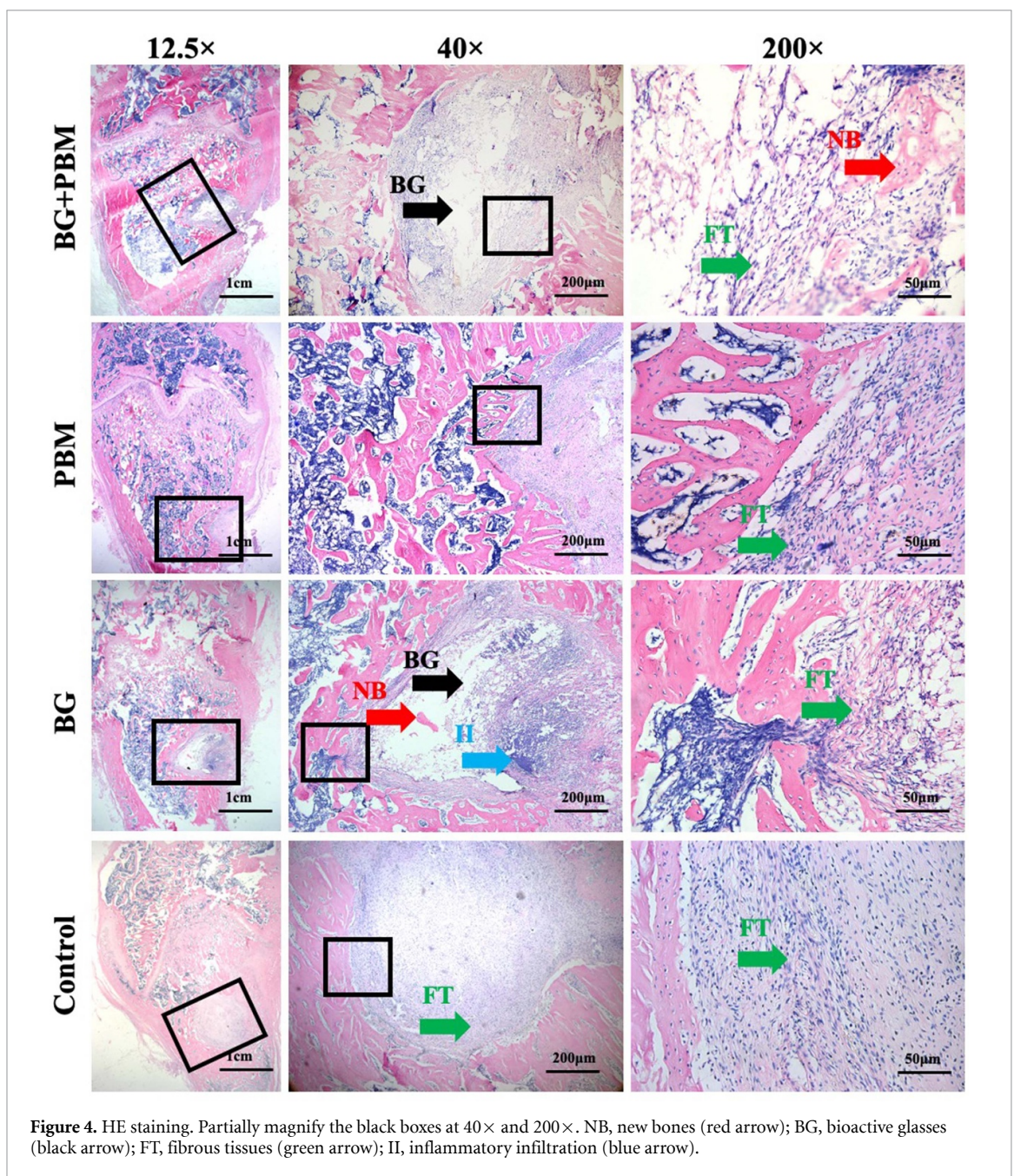
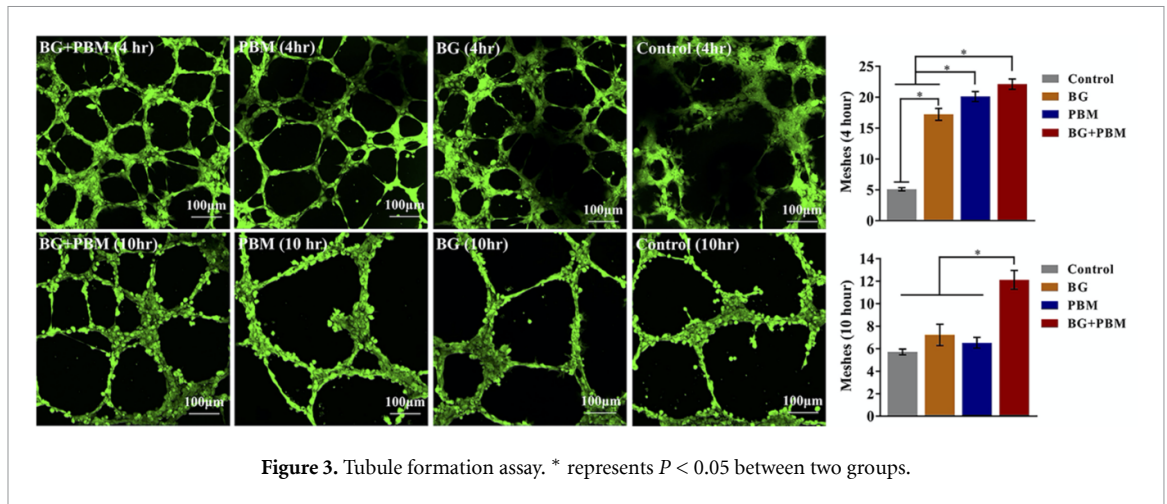
3.4. PBM combined with BG increased vascular-like structure formation *in vivo*

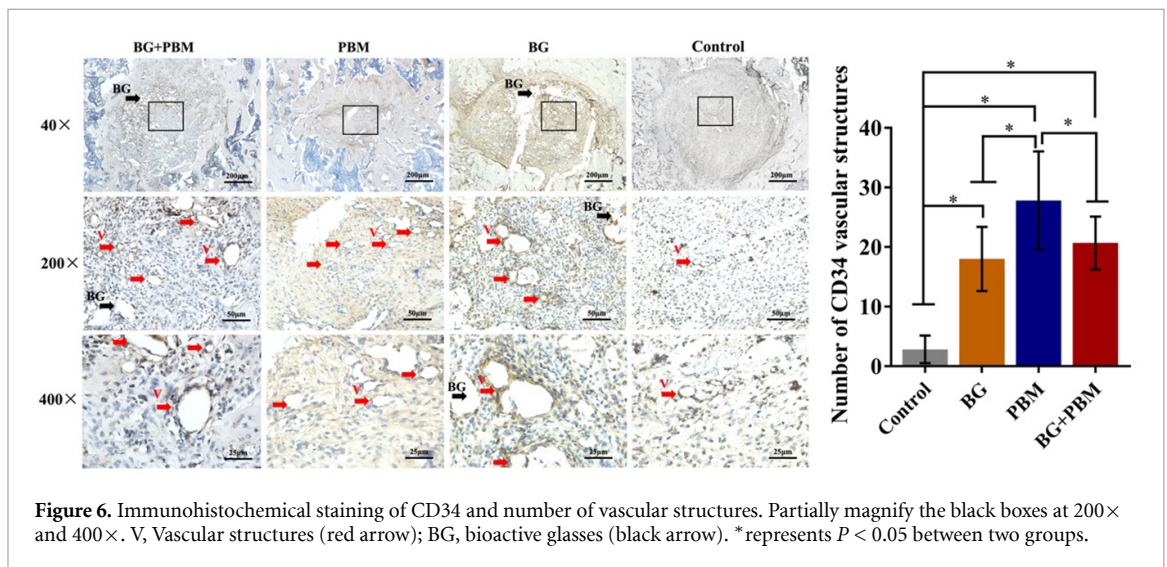
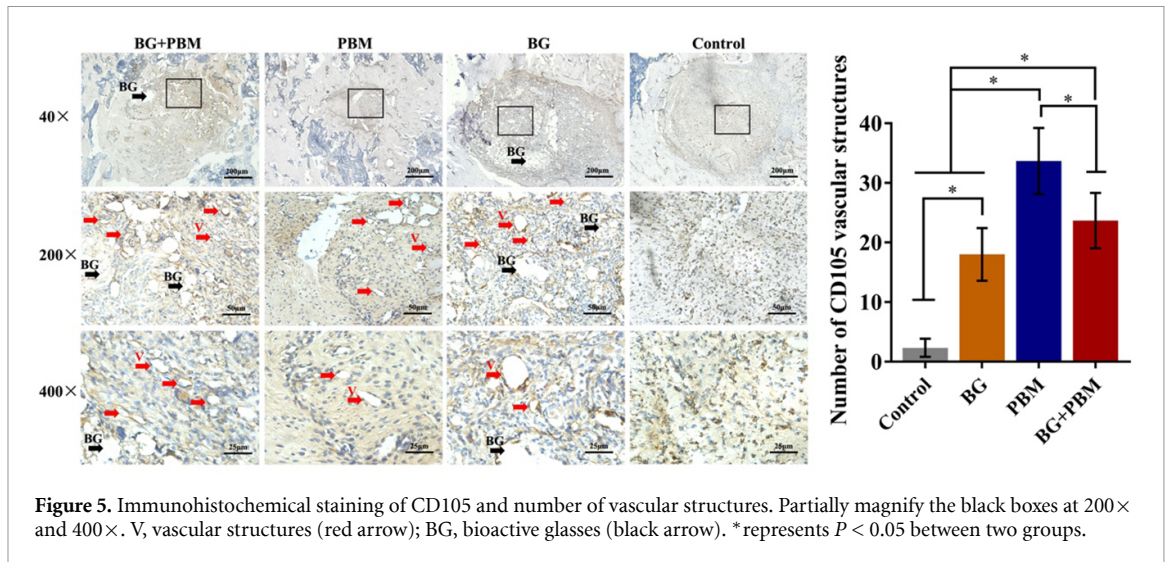
The postoperative recovery and diet of rats in all the groups were normal and the incisions healed well without inflammatory reactions. The weights of the rats were approximately 530 g two weeks after the surgery. Then, the specimens were obtained, and HE staining and immunohistochemical staining were performed.

HE staining was used to observe the inflammatory response, tissue formation and biomaterial absorption of bone defects. At 2 weeks post-surgery, the

results showed that there was fibrous matrix in the defect of all groups and obvious inflammatory infiltration were found in the BG group. Cavities could be observed in the BG + PBM group and BG group, as large amount of undegraded BG particulates demineralized. In the BG + PBM group and BG group, a small number of scattered new bone tissues were observed inside the defects (figure 4).

CD105 and CD34 immunohistochemical staining were used to observe the vascular-like structures in the center of bone defects. The cytoplasm of vascular endothelial cells was stained brown and the cell





nucleus was stained blue or purple. The independent and complete lumen formed by stained endothelial cells was considered as the vascular-like structure. The observation of slices revealed that BG particulates were wrapped by fibrous tissues, while the edge of demineralized cavities could also be stained brown, but the shape of such structures was irregular and incomplete, which could be distinguished from the vascular-like structures.

In the center of bone defects, CD105 staining was enhanced in the BG + PBM and PBM groups, while very few brown staining was observed in the control group. The results of quantitative analysis showed that the most vascular structures were formed in the PBM group (33.67 ± 5.559) among all the groups with statistical significance ($P < 0.01$). More vascular structures formed in the BG + PBM group (23.67 ± 4.633) than in the BG group (18.00 ± 4.427) ($P = 0.016$) and control group (2.33 ± 1.506) ($P < 0.01$) (figure 5).

Quantitative analysis of CD34 expression revealed that the vascular structures in the PBM group

(27.83 ± 8.208) was significantly increased compared with the BG + PBM group (20.67 ± 4.457) ($P = 0.036$), the BG group (18.00 ± 5.367) ($P < 0.01$) and the control group ($P < 0.01$) (figure 6).

4. Discussion

Angiogenesis is essential for wound healing and tissue regeneration. Promote angiogenesis to facilitate osteogenesis has always been a key challenge. Concomitant blood vessels play a vital role in supplying oxygen and nutrients to newly formed tissues, eliminating metabolites, delivering growth factors and providing key signals for bone metabolism [30]. Insufficient early angiogenesis will hinder the biomaterial fusion and absorption with tissues, and then hindering the bone regeneration [12, 13]. Some studies have demonstrated the effect of BG on promoting angiogenesis [31–33], but the early proangiogenic capacity of BG, especially the early angiogenesis in large-sized bone defects filled with BG, needs more studies [9–11]. To improve the early angiogenesis,

much effort has been spent on the improvement of materials' optimization of the composition and morphology, such as coating inorganic ions (copper, strontium, cobalt) [34–36], and modifying the porosity and pore size of scaffolds [37–39]. However, this may also lead to some problems. Firstly, toxic effects on cells may exist due to the dosage and burst release of trace elements [40]. Acute inflammatory response after biomaterial implantation will also cause undesired effects on early angiogenesis [10, 11]. Secondly, although higher porosity and macroporosity of scaffold materials are beneficial for tissue growth [37–39], oversized pores will hamper the bio-physicochemical and mechanical properties of materials, further affecting ion release, cell adhesion and signal pathway activation [37, 39]. In this study, we considered PBM as an alternative approach and applied with BG aiming to exert additive effects to improve the early angiogenesis of BG in bone regeneration.

PBM therapy has been widely performed in tissue engineering as a physical method. It applies various light sources in the wavelength from visual to infrared to activate endogenous photoreceptors and generate biological effects [41, 42]. Studies have shown that lights with wavelength from 600 to 1000 nm may be able to activate mitochondria, increase mitochondrial-derived reactive oxygen species and calcium, promote ATP production and initiate a series of cascade reactions [42, 43]. Moreover, lasers with wavelengths ranging from 650 to 950 nm exert the most effective role in tissues with a penetrating depth of 2–3 mm, which is suitable for deep injuries [44, 45]. Considering the biological stimulation effects and tissue-penetration ability, we used 808 nm-wavelength near-infrared laser and combined it with BG in the present study to examine their effects on early angiogenesis *in vitro* and *in vivo*.

First, we assessed the effects of PBM combined with BG on pro-angiogenic genes expression and tubule formation *in vitro*. The results showed that PBM upregulated VEGF and bFGF genes expression during the early stage. When HUVECs were treated with the combination of PBM and BG, the mRNA levels showed earlier and significantly higher expression than those of other groups. In the tubule formation assay, the PBM treatment accelerated HUVEC tubule formation. The BG + PBM and PBM groups both formed more mature tubules at 4 h. The tubules in the BG + PBM group were significantly greater than other groups at 10 h. Above results revealed that the combination of PBM and BG exhibited the strongest promotion on angiogenic-related genes activation and HUVEC angiogenesis. The mechanism might have two aspects. On one hand, PBM exhibited the good ability to initiate angiogenic process rapidly and promote early angiogenesis, which was consistent with previous studies. PBM has been reported to

promote eNOS synthesis, activate PI3K, MAPKs and other signal pathways, increase VEGF and bFGF levels, and further promote endothelial cells proliferation, migration and angiogenesis [18, 19]. On the other hand, the angiogenic effect of PBM was enhanced by BG. The combination of PBM and BG produced an additive effect on angiogenesis which was superior to applying either BG or PBM individually. When contacting with the body fluid, BG particulates release large amount of Si ions, which upregulates the expression of angiogenic growth factors and receptors, stimulates eNOS synthesis and further regulates cells migration as well as vasculature formation [7, 8].

We further investigated the early angiogenic effects of PBM combined with BG *in vivo* and observed vascular-like structures formation by immunohistochemical assay. CD105 is widely expressed in endothelial cells of microvascular system and is specific in detecting neovascularization [46]. CD34 is also a major marker of mature vascular endothelial cells widely used in clinic [47]. The immunohistochemical results were consistent with the *in vitro* results, showing that PBM promoted the formation of vascularized tissues in the new bone as well as the central area of bone defects. The combination of PBM and BG significantly improved early angiogenic levels compared to applying BG only. These results suggested that PBM enhanced angiogenesis in BG-filled bone defects. As for the BG + PBM group exhibited less vascular structures than the PBM group, the reason may be that the BG particulates occupied most of the bone defects space in the BG + PBM group, resulting in less soft tissues volume which contained blood vessels. However, there was more soft tissue volume in the PBM group, which resulted in more blood vessels in the quantitative analysis. Moreover, although we found a clear trend between groups, the standard deviations of our results were relatively large, indicating that there may be differences among individuals. Therefore, more experiments and samples should be considered in our further study for achieving stable results.

Our study preliminarily explored the effects of PBM combined with BG on early angiogenesis. The results suggested PBM combined with BG exhibited an additive effect on early angiogenesis, which may be favorable for tissue regeneration. Meanwhile, by reducing the use of chemicals, the addition of PBM will be beneficial for minimizing the potential risk of biological safety caused by the dosage and burst release of trace elements [40]. Moreover, the role of PBM in reducing inflammatory response can also reduce the acute inflammatory response after biomaterial implantation, which plays an important role in early angiogenesis [10, 11, 48]. Therefore, our study preliminarily confirmed the feasibility of this combination. For clinical application, the additive

effects of PBM and BG on angiogenesis as well as the good biocompatibility of PBM may provide an improvement for bone regeneration and bone defects repair.

Our study also emphasized the importance of PBM and BG dosages, and only in an appropriate condition could we observe the enhancement in cell growth and tissue regeneration. A recent review [49] included 16 literatures on the effects of PBM and biomaterials on tissue regeneration. It was found in 75% of the studies that ceramic biomaterials and infrared PBM presented positive effects on the process of bone defect healing. The main reason for the negative results in the other studies was probably the excess of stimulus to tissue, which was in association with the dosage of PBM and BG.

The effect of PBM is dose-dependent, in which both low and high doses might result in inhibition while moderate doses induce cells activity [44]. Therefore, we first investigated the effect of PBM with different fluences on HUVEC proliferation to determine the optimum dose of PBM *in vitro*. At the same time, to avoid the harmful ‘energy accumulation effect’ [50], we conducted fractional irradiation in which PBM therapy was performed 3 times in total with intervals of 24 h rather than intense applications over a short period of time. This intermittent irradiation avoided the overload of intracellular calcium, which may cause a rapid cellular energy consumption and even cell death [50]. Comparing to *in vitro* situation, the PBM fluence of *in vivo* should be higher. For one reason, bones and bone marrow are tissues deep within the body and have lower numbers of mitochondria [51]. And it is more likely for tissue with lower mitochondria to be ineffective due to under-dosing rather than over-dosing [51]. Another reason was that skin, muscle, and other tissues will weaken part of the light energy and penetration depth [45, 52]. There is still no agreement on the parameters and protocols for the application of PBM. Positive effects using the fluence of 140 J cm^{-2} on bone repair have been reported, and we set the PBM fluence at 120 J cm^{-2} with reference to previous literature and former experience [51]. Considering the complexity and diversity of organisms, suitable doses of PBM for *in vivo* application still need to be studied.

The regulation of BG on cell activities is also dose-dependent, and ions play a positive biostimulation role with appropriate concentrations while high concentrations will cause cytotoxicity [53, 54]. In order to create a cell-friendly environment in *in vitro* studies, first of all, we set gradient concentrations of BG extracts to select an optimum dose for cell growth, ensuring suitable number of ions can be used for cell activities. In addition, the pre-conditioning of BG is important, as alkaline ions ‘burst release’ occurs when BGs rapidly exchange ions with surrounding medium, leading to an undesired increase of pH and unfavorable effects on cell function and activity [55].

Therefore, 24 h pre-incubation of BG was applied in our study to reduce the rate of ions release and limit pH excursion. What’s more, PSC, the biomaterial used in our study possesses a higher phosphorus content compared to 45S5 Bioglass® (wt%: 6% P_2O_5 -45% SiO_2 -24.5% CaO -24.5% Na_2O), which limits the pH change around PSC particulates to a narrower range during dissolution [29, 56, 57]. Another study [29] compared pH changes of PSC and 45S5 at different concentrations and showed that at 1 mg ml^{-1} , there was a sudden increase in the pH of 45S5 from 7.45 to 8.11 in the first hour, while the pH of PSC increased slightly from 7.45 to 7.62. At 1 mg ml^{-1} and higher concentration, 45S5 extracts displayed a notably increased pH from 7.66 to 8.84 after 24 h incubation, while PSC extracts showed a significant increase in pH at 4 mg ml^{-1} and remained stable at approximately 7.8. The above results confirmed that low concentrations of PSC extracts would not cause notable increases in pH, which created a more stable and cell-friendly pH microenvironment for cell activity.

There were still some problems to be solved in further studies, such as the mechanism of additive effects of PBM and BG, the energy attenuation of PBM in tissue, the optimal combined parameters of PBM and BG *in vivo*, the effects of PBM and BG on tougher clinical situations like osteoporosis related fractures and large fractures, etc. In further studies, we will make efforts in the above aspects to better apply PBM and BG in bone defects repair.

5. Conclusions

The combination of PBM and BG generated additive effects on promoting early angiogenesis both *in vitro* and *in vivo*, representing a promising and biologically safe method to improve the bone defects repair. The effect of PBM and BG is dose- and concentration-dependent. Therefore, it is necessary to determine the appropriate parameters to ensure PBM and BG exert their optimal additive effects.

Data availability statement

All data that support the findings of this study are included within the article (and any supplementary files).

Acknowledgments

This work has been supported by the National Natural Science Foundation of China [Project 81870753] and Peking University School of Stomatology [Project PKUSS20190104]. Thanks to Professor Dong Qiu and his research group in the Institute of Chemistry, Chinese Academy of Sciences for providing bioactive glasses for this study. Lidong Huang and Weiyu Gong contributed equally to this study and share the first authorship.

Author contributions

Lidong Huang (first author): Methodology, Formal analysis, Data curation, Investigation, Writing-Original draft preparation, Writing-review & editing, Visualization. Weiyu Gong (co-first author): Methodology, Validation, Supervision, Writing-review & editing, Funding acquisition, Resources. Guibin Huang: Investigation. Jingyi Li: Investigation. Jilin Wu: Investigation. Yuguang Wang (co-corresponding author): Methodology, Resources. Yanmei Dong (corresponding author): Conceptualization, Methodology, Funding acquisition, Resources, Supervision, Writing-review & editing.

ORCID iD

Lidong Huang  <https://orcid.org/0000-0003-3347-6091>

References

- [1] Hench L L, Xynos I D and Polak J M 2004 *J. Biomater. Sci. Polym. Ed.* **15** 543–62
- [2] Allison D C, McIntyre J A, Ferro A, Brien E and Menendez L R 2013 *Curr. Orthop. Pract.* **24** 267–79
- [3] Moore W R, Graves S E and Bain G I 2001 *ANZ J. Surg.* **71** 354–61
- [4] Strocchi R, Orsini G, Iezzi G, Scarano A, Rubini C, Pecora G and Piattelli A 2002 *J. Oral. Implantol.* **28** 273–8
- [5] Keles G C, Cetinkaya B O, Albayrak D, Koprulu H and Acikgoz G 2009 *Acta Odontol. Scand. Suppl.* **64** 327–33
- [6] Stanley H R, Hall M B, Clark A E, King C J 3rd, Hench L L and Berte J J 1997 Using 45S5 bioglass cones as endosseous ridge maintenance implants to prevent alveolar ridge resorption: a 5-year evaluation *Int. J. Oral. Maxillofac. Implants* **12** 95–105
- [7] Li H and Chang J 2013 *Acta Biomater.* **9** 5379–89
- [8] Zhang M, Chen X, Pu X, Liao X, Huang Z and Yin G 2017 *J. Biomed. Mater. Res. A* **105** 3159–68
- [9] Mao C, Chen X, Miao G and Lin C 2015 *Biomed. Mater.* **10** 025005
- [10] Chen Z, Klein T, Murray R Z, Crawford R and Yin X 2016 *Mater. Today* **19** 304–21
- [11] Loi F, Córdova L A, Pajarinen J, Lin T-H, Yao Z and Goodman S B 2016 *Bone* **2016** 119–30
- [12] Santos M I and Reis R L 2010 *Macromol. Biosci.* **10** 12–27
- [13] Lee S-H, Coger R N and Clemens M G 2006 *Tissue Eng.* **12** 2825–34
- [14] Anders J J, Lanzafame R J and Arany P R 2015 *Photomed. Laser Surg.* **33** 183
- [15] Alghamdi K M, Kumar A and Moussa N A 2012 *Lasers Med. Sci.* **27** 237–49
- [16] Chen C-H, Hung H-S and Hsu S-H 2010 *Lasers Surg. Med.* **40** 46–54
- [17] Szymanska J et al 2013 Phototherapy with low-level laser influences the proliferation of endothelial cells and vascular endothelial growth factor and transforming growth factor-beta secretion *J. Physiol. Pharmacol.* **64** 387–91
- [18] Webb C, Dyson M and Lewis W H 2015 *Lasers Surg. Med.* **22** 294–301
- [19] Huang Y-Y, Sharma S K, Carroll J and Hamblin M R 2011 *Dose-Response* **9** 602–18
- [20] Bellato C P, Oliveira D L D, Kasaya M V S, Moreira D and Santos P L 2021 *Acta Cir. Bras.* **36** e360603
- [21] Bossini P S, Rennó A C M, Ribeiro D A, Fangel R, Peitl O, Zanotto E D and Parizotto N A 2015 *J. Tissue Eng. Regen. Med.* **5** 229–37
- [22] Lopez T C C et al 2017 *J. Biomed. Mater. Res. B* **105** 107–16
- [23] Mendonça F A, Marques M, Cavalcanti S C S X B, Pedroni A C F and Lascala C A 2020 *J. Photochem. Photobiol. B* **213** 112053
- [24] Magri A M P et al 2019 *J. Mater. Sci. Mater. Med.* **30** 105
- [25] Guilherme M et al 2018 *Int. J. Oral. Maxillofac. Implants* **33** 169–74
- [26] Oliveira P, Ribeiro D A, Pipi E F, Driusso P, Parizotto N A and Renno A C M 2010 *J. Mater. Sci. Mater. Med.* **21** 1379–84
- [27] Pinto K N Z et al 2013 *Photomed. Laser Surg.* **31** 252–60
- [28] Li A and Qiu D 2011 *J. Mater. Sci. Mater. Med.* **22** 2685–91
- [29] Cui C, Wang S, Ren H, Li A, Qiu D, Gan Y and Dong Y-M 2017 *RSC Adv.* **7** 22063–70
- [30] Rouwkema J and Khademhosseini A 2016 *Trends Biotechnol.* **34** 733–45
- [31] Kargozar S, Baino F, Hamzehlou S, Hill R G and Mozafari M 2018 *Trends Biotechnol.* **36** 430
- [32] Day R M 2005 *Tissue Eng.* **11** 768
- [33] Gorustovich A A, Roether J A and Roether J A 2010 *Tissue Eng. B* **16** 199–207
- [34] Zhao F, Lei B, Li X, Mo Y, Wang R, Chen D and Chen X 2018 *Biomaterials* **178** 36–47
- [35] Zhou Y, Han S, Xiao L, Han P, Wang S, He J, Chang J, Wu C and Xiao Y 2018 *J. Mater. Chem. B* **6** 3274–84
- [36] Wang X et al 2019 *ACS Biomater. Sci. Eng.* **5** 4496–510
- [37] Baino F, Fiorilli S and Vitale-Brovarone C 2016 *Acta Biomater.* **42** 18–32
- [38] Druce D, Langer S, Lamme E, Pieper J, Ugarkovic M, Steinau H U and Homann H H 2010 *J. Biomed. Mater. Res. A* **68A** 10–18
- [39] Nguyen L H, Annabi N, Nikkiah M, Bae H, Binan L, Park S, Kang Y, Yang Y and Khademhosseini A 2012 *Tissue Eng. B* **18** 363–82
- [40] Gentleman E, Fredholm Y C, Jell G, Lotfibakhshahi N, O'Donnell M D, Hill R G and Stevens M M 2010 *Biomaterials* **31** 3949–56
- [41] Karu T 1999 *J. Photochem. Photobiol. B* **49** 1–17
- [42] Karu T 2008 *Photochem. Photobiol.* **84** 1091–9
- [43] Moore P, Ridgway T D, Higbee R G, Howard E W and Lucroy M D 2005 *Lasers Surg. Med.* **36** 8–12
- [44] Avci P, Gupta A, Sadasivam M, Vecchio D, Pam Z, Pam N and Hamblin M R 2013 Low-level laser (light) therapy (LLLT) in skin: stimulating, healing, restoring *Semin. Cutan. Med. Surg.* **32** 41–52
- [45] Chung H, Dai T, Sharma S K, Huang Y, Carroll J D and Hamblin M R 2012 *Ann. Biomed. Eng.* **40** 516–33
- [46] Reinmuth N, Thomas M, Meister M, Schnabel P A and Kreuter M 2010 *Eur. Res. J.* **36** 915–24
- [47] Wikström P, Lissbrant I F, Stattin P, Egevad L and Bergh A 2002 *Prostate* **51** 268–75
- [48] Hamblin M R 2017 *AIMS Biophys.* **4** 337–61
- [49] Magri A M P, Parisi J R, Andrade A L M D and Rennó A C M 2021 *J. Biomed. Mater. Res. A* **109** 1765–75
- [50] Sommer A P, Pinheiro A L, Mester A R, Franke R P and Whelan H T 2001 *J. Clin. Laser Med. Surg.* **19** 29–33
- [51] Zein R, Setting W and Hamblin M R 2018 *J. Biomed. Opt.* **23** 1–17
- [52] Barolet D 2008 *Semin. Cutan. Med. Surg.* **27** 227–38
- [53] Maeno S, Niki Y, Matsumoto H, Morioka H, Yatabe T, Funayama A, Toyama Y, Taguchi T and Tanaka J 2005 *Biomaterials* **26** 4847–55
- [54] Shie M Y, Ding S J and Chang H C 2011 *Acta Biomater.* **7** 2604–14
- [55] Ciraldo F E, Boccardi E, Melli V, Westhauser F and Boccaccini A R 2018 *Acta Biomater.* **75** 3–10
- [56] Li A et al 2011 *J. Non-Cryst. Solids* **357** 3548–55
- [57] Li A, Lv Y, Ren H, Cui Y and Qiu D 2017 *Int. J. Appl. Glass Sci.* **8** 403–11